J Fluoresc (2007) 17:547–563
DOI 10.1007/s10895-007-0210-4

ORIGINAL PAPER

Water Soluble Metallo-Phthalocyanines: The Role of the Functional Groups on the Spectral and Photophysical Properties

Vera T. Verdree · Serhii Pakhomov · Guifa Su · Michael W. Allen · Amber C. Countryman · Robert P. Hammer · Steven A. Soper

Received: 16 November 2006 / Accepted: 16 May 2007 / Published online: 16 June 2007

Abstract Strategies are reported that produce symmetrical metal-free and metallo-phthalocyanine dyes, Pc and MPc, respectively, containing various numbers of water solubilizing carboxylic acid groups on their periphery that provide a dual role by also serving as functional groups to covalently link primary amine-containing targets to these dyes. In order to induce water compatibility and to minimize the degree of aggregation, the periphery of the macrocycle was decorated with various numbers of water-solubilizing groups and/or altering the identity of the metal center. The influence of the number of solubilizing groups and metal center on the spectral and photophysical properties were evaluated. MPc dyes containing 4, 8, or 16 carboxylic acid groups exhibited similar absorption and emission maxima (677 and 686 nm, respectively) with the molar absorptivity of the Q-band ~10^5 M^{-1} cm^{-1}. Results indicated that the fluorescence lifetimes and quantum yields varied as a function of the metal center; the degree of carboxylation did not significantly alter these properties in DMSO, but did mediate the solubility and aggregation states when placed in aqueous solvents. The water solubilizing groups could also serve as labeling moieties for targets bearing primary amines. Results showed that the conjugate, produced by covalently linking an MPc to streptavidin through one of its carboxylate groups, generated a red-shift in the emission maximum with a fluorescence lifetime shorter than that of the native MPc dye.

Keywords Metal phthalocyanine · Near-IR fluorescence · Bioconjugation · Photophysics

V. T. Verdree · S. Pakhomov · G. Su · M. W. Allen · A. C. Countryman · R. P. Hammer · S. A. Soper
Department of Chemistry, Louisiana State University, Baton Rouge, LA 70803, USA

S. A. Soper
Department of Mechanical Engineering, Louisiana State University, Baton Rouge, LA 70803, USA

Present Address:
G. Su
College of Chemistry and Chemical Engineering, Guangxi Normal University, Guilin 541004, China

Present Address:
M. W. Allen
Thermo Electron Corporation, 5225 Verona Road, Madison, WI 53711, USA

Present Address:
S. A. Soper (✉)
Room 229, Choppin Hall,
Baton Rouge, LA 70803, USA
e-mail: chsope@lsu.edu

Introduction

Phthalocyanines (Pc) and their metal complexes (MPc) have attracted considerable interest and have been found to be highly promising candidates for a variety of uses such as liquid crystals [1, 2], photosensitizers [3–5], and in various chemical sensing applications [6, 7]. The properties that make Pc/MPc dyes particularly attractive as potential bioassay reagents include their high molar absorptivity [8, 9], resistance to chemical and photochemical degradation [10], absorption and emission in the deep red region of the electromagnetic spectrum [9, 10], long lifetimes with high quantum yields [10], and a wide range of accessible chemical structures allowing the design of compounds

capable of meeting certain needs [11]. The difficulties associated with these dyes includes their propensity to form aggregates due to molecular stacking resulting in low quantum yields [12, 13], limited solubility in aqueous media, formation of mixed isomers during synthesis [14, 15] and difficulties in purifying these dyes to homogeneity using standard chromatographic methods [16]. Unfortunately, these limitations have severely limited the use of Pc and MPc dyes as potential labeling reagents for ultrasensitive fluorescence-based measurements.

MPc's and Pc's are chemically robust and photochemically stable due in part to the nitrogens located within the aromatic macrocycle and the peripherally fused benzene rings [17, 18]. These dyes possess a strong absorption band in the near-IR due to the extended π-conjugation system around the ring structure [3, 10]. Pc's can coordinate a variety of metals in their central cavity, which further enables tailoring their spectral and photophysical properties because the metal can affect the pathways of the excited MPc returning to the ground state, in particular the rate of intersystem crossing resulting from metal-ligand spin-orbit coupling [19, 20]. In addition, interaction of the metal with the π system of the Pc can modify the electron distribution of the macrocycle resulting in additional absorption bands and/or bathochromic shifts in existing bands, which are highly dependent upon the paramagnetic properties of the central metal.

Several examples have appeared in the literature in which Pc derivatives have been described with emphasis placed on the synthesis of the Pc with a primary goal of tuning the water solubility and aggregation effects [21, 22]. For example, Liu et al. [5] reported on the synthesis of ZnPc's bearing 16-carboxylic acids to reduce aggregation for use as a potential photosensitizer for cancer therapy. Ng et al. [23] synthesized dendritic phthalocyanines and studied their aggregation behavior, which was influenced by interactions with surfactants. Margaron et al. [4] synthesized several different ZnPc dyes to evaluate their use for photodynamic therapy. Results indicated that the phototoxicity increased with decreasing number of sulfonate groups on the periphery. Sener [24] reported on the synthesis and spectroscopic studies of MPc's substituted with dicarboxyethyl substituents designed to control intermolecular dimerization of the MPc's in solution. Spectroscopic evaluation indicated a high propensity of these compounds to dimerize at pH>6.

Unfortunately, none of the aforementioned work described the role of the solubilizing groups on the photophysical properties of the MPc or Pc dyes or has used the peripheral water solubilizing groups (i.e., symmetrical Pc dyes) as an attachment scaffold to biomolecular targets. Several groups have reported the use of asymmetrical MPc derivatives as fluorescent labeling reagents bearing a single isothiocyanato group for tagging monoclonal antibodies or oligonucleotides [25, 26]. Asymmetrical MPc's, which are comprised of water solubilizing groups and a functional group, however, are difficult to prepare and isolation of the desired product is often challenging as a result of statistical mixtures of substituted Pc's obtained during synthesis.

Herein, we report on the synthesis, spectroscopic and photophysical properties of several symmetrical Pc's and MPc's that can potentially serve as fluorogenic labeling reagents for near-IR fluorescence applications that exhibit favorable water solubility, minimal aggregation effects in aqueous media and facile conjugation routes to primary-amine containing targets. We made use of symmetrical MPc's as the labeling reagents for conjugation due to their ease of preparation and simplified purification methods. We examined alkoxy substituted MPc's having peripheral four, 8 and 16 carboxylate groups and a variety of central metal ions (Al(OH), Ga(OH), Zn, Ni, Pt and Pd) as well as metal-free Pc's in order to evaluate the spectroscopic and photophysical effects of these substitutions on the base chromophore and aggregation properties. These water solubilizing groups were also used for the covalent attachment of biomolecules to the fluorophore. Fluorescence quantum yields, radiative lifetimes and photobleaching quantum yields, which are crucial in determining the feasibility of using any dye as reporters for high sensitivity analyses of biological molecules, will be reported and related to the degree of carboxylation of the MPc. In addition, the spectral and photophysical properties will be examined upon conjugating an MPc dye to a biological target (i.e., streptavidin).

Experimental

Materials Spectral grade dimethyl sulfoxide (DMSO) and dimethylformamide (DMF) were obtained from Aldrich Chemical Co. (Milwaukee, WI). *N*-hydroxysuccinimide ester (NHS), and *N*,*N*-dicyclohexylcarbodiimide (DCC) was purchased from Sigma-Aldrich Co. (Milwaukee, WI). 3-(Cyclohexylamino)-1-propanesulfonic acid (CAPS) and 4-(2-Hydroxyethyl) piperazine-1-ethanesulfonic acid (HEPES) were obtained from Sigma. HPLC grade acetonitrile was purchased from Aldrich Chemical Co. and used without further purification. Triethylammonium acetate (TEAA) buffer and streptavidin from streptomyces avidinii were purchased from Fluka (St. Louis, MO). Zinc acetate and nickel acetate tetrahydrate were finely ground, dried at 110°C under vacuum for 30 h and stored in sealed vials; palladium (II) chloride, platinum (II) chloride, anhydrous aluminum chloride, anhydrous gallium chloride, anhydrous tin (IV) chloride were used as received.

Purification and identification methods Chromatographic separations were obtained using a Jasco HPLC (Jasco, Inc., Easton, MD) equipped with a diode array and fluorescence detector. Reverse-phase HPLC chromatography was performed using a Supelco C-18 column (Bellefonte, PA) with a linear gradient of 5–95% acetonitrile/0.1% TEAA for 45 min at a flow rate of 1 ml/min. Analysis of the HPLC data was performed using EZChrom software provided by JASCO. The purity of MPc's was verified through the observance of a single peak when monitored at 680 nm. Thin layer chromatography (TLC) was performed using silica gel as the stationary phase. Flash chromatography was performed with silica gel of particle size 60 μm. Melting points were determined using a Fisher–Johns melting point apparatus. NMR spectra were recorded on a Bruker DPX-250. GC-MS spectra were recorded on a Hewlett Packard 5971A mass spectrometer in EI mode at 70 eV. MALDI mass spectra were recorded on a Bruker ProFLEX III MALDI-TOF mass spectrometer.

Synthesis of substituted phthalonitriles (**1**–**3**) A mixture of 4-nitrophthalonitrile (for the synthesis of **1**, see Scheme 1), 4,5-dichlorophthalonitrile (7 mmol, for the synthesis of **2** and **3**, see Schemes 2 and 3, respectively), substituted 4-hydroxybenzoate (for **1**, 7.5 mmol and for **2** and **3**, 15.4 mmol) and dried potassium carbonate (6.38 g, 46.2 mmol) in anhydrous DMF (50 ml) was stirred overnight at 85°C in an inert atmosphere. After cooling to room temperature, the mixture was diluted with ethyl acetate (60 ml) and water (40 ml). The organic layer was separated and the aqueous phase was extracted with ethyl acetate (2×50 ml). The combined organic layers were washed with a saturated solution of $NaHCO_3$ (40 ml), brine (40 ml) and dried over Na_2SO_4. The solvents were removed in vacuo, and the crude product was purified by column chromatography on silica gel using dichloromethane/acetonitrile mixture (20:1) as an eluent to furnish **1**–**3**.

4-(4-Pentoxycarbonyl) phenoxyphthalonitrile (**1**) Yield: 88%, mp 48–49°C, ^{1}H NMR ($CDCl_3$) δ 8.15 (d, 2H, J=8.7 Hz), 7.77 (d, 1H, J=8.7 Hz), 7.35 (d, 1H, J=2.3 Hz), 7.30 (d, 1H, J=8.7 Hz), 7.12 (d, 2H, J=8.7 Hz), 4.34 (2H, t, OCH_2, J=6.7 Hz), 1.79 (m, 2H, CH_2), 1.42 (m, 4H, CH_2CH_2), 0.94 (t, 3H, J=7 Hz, CH_3).

4,5-Bis(4-pentoxycarbonyl) phenoxyphthalonitrile (**2**) Yield: 88%, mp 77–78°C, ^{1}H NMR ($CDCl_3$) δ 8.11 (dd, 4H,

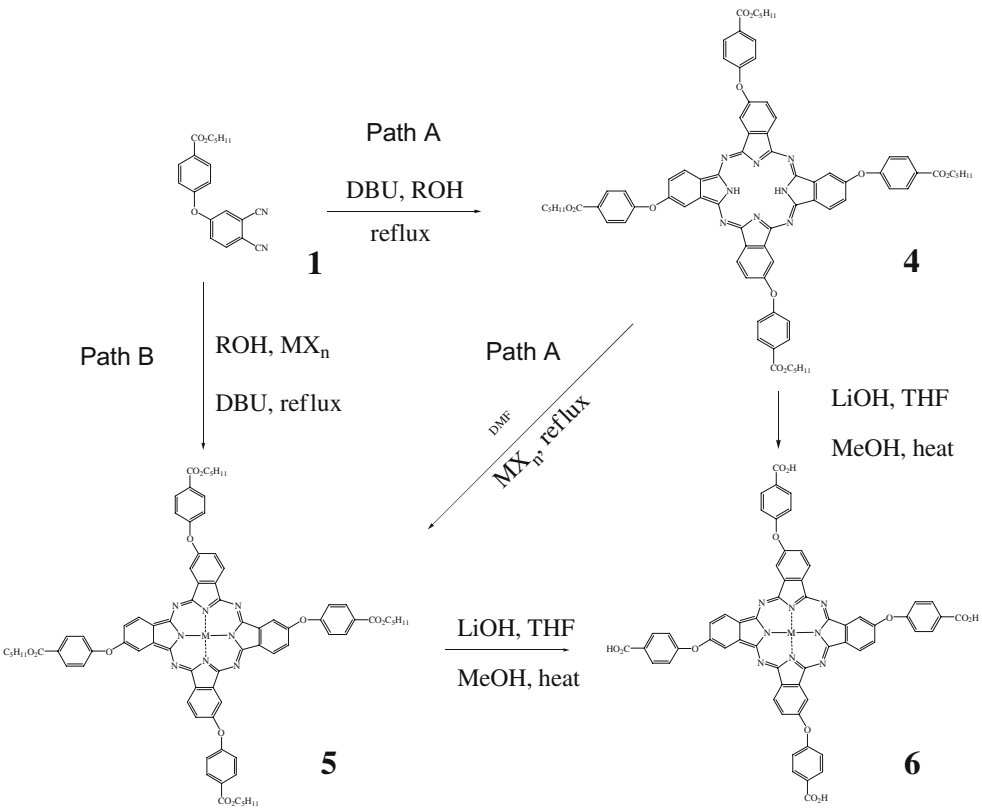

Scheme 1 Synthesis of 2,9,16,23-tetrasubstituted Pc's

Esters M = Zn, **5a**; GaCl, **5b**; AlCl, **5c**; Ni, **5d**; Pd, **5e**; Pt, **5f**

Tetracarboxylates M = Zn, **6a**; GaOH, **6b**; AlOH, **6c**; Ni, **6d**; Pd, **6e**; Pt, **6f**; 2H, **6g**

Scheme 2 Synthesis of 2,3,9,10,16,17,23,24-octasubstituted Pc's

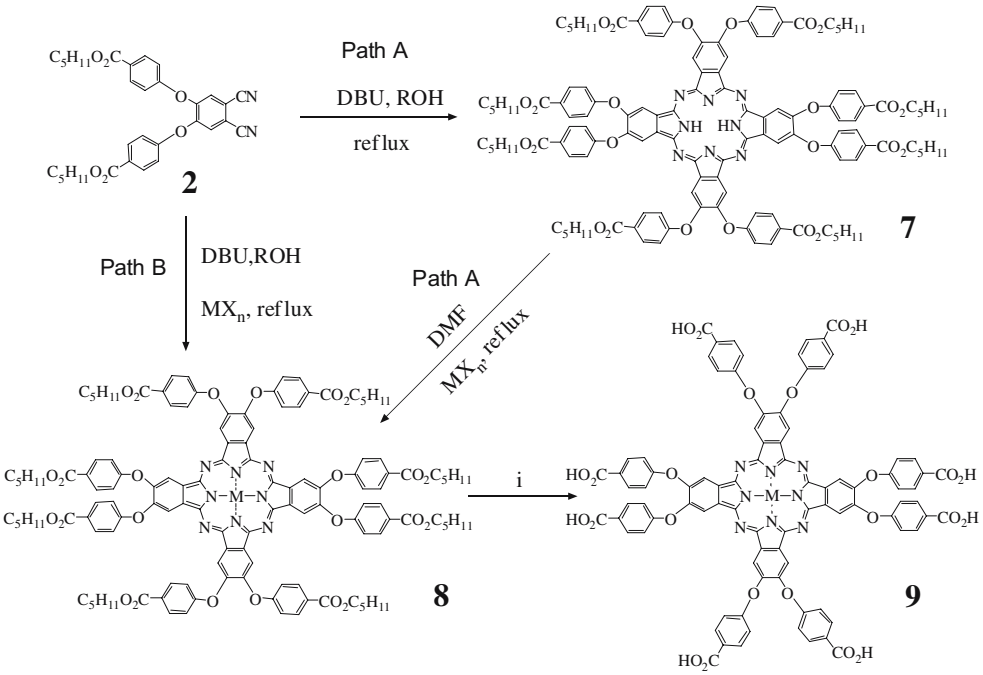

Scheme 3 Synthesis of 2,3,9,10,16,17,23,24-octasubstituted hexadeca functionalized Pc's

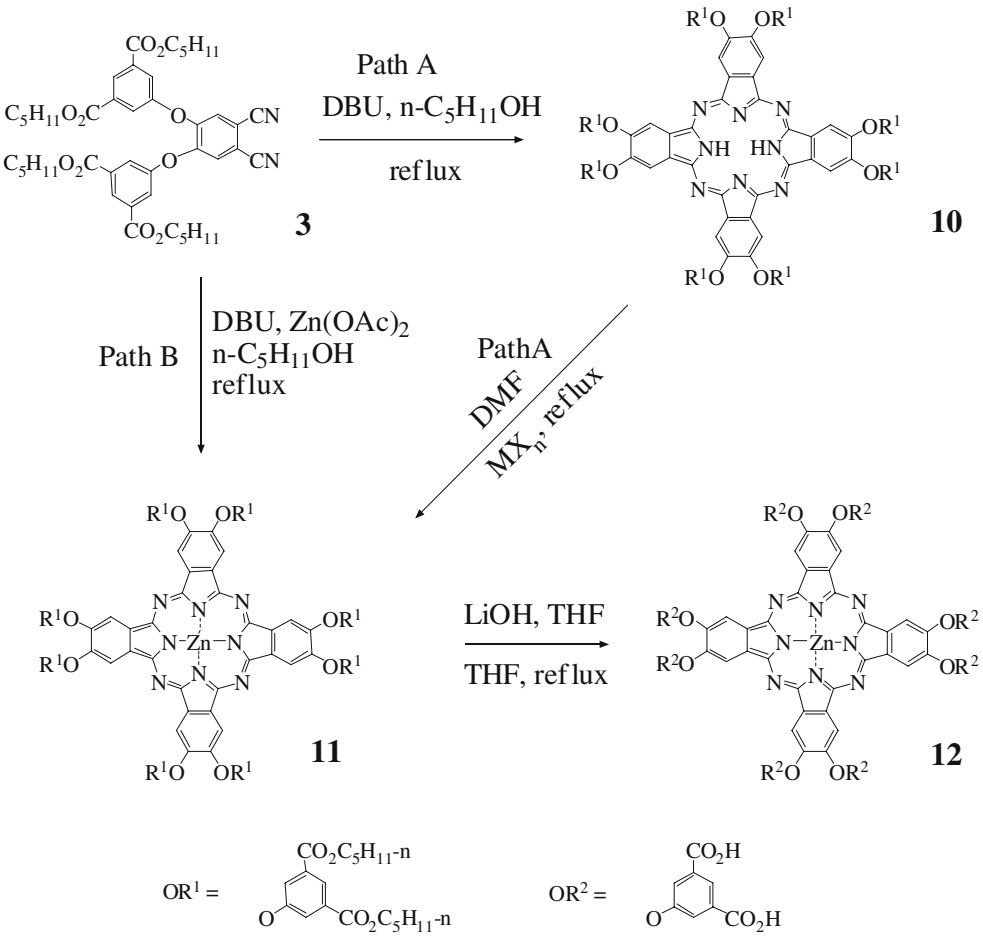

Table 1 Absorption (λ_a) and emission (λ_e) maxima of a metal free (H_2Pc) and several MPc dyes

Compound	λ_a[a] (nm)	λ_f[a] (nm)	ε[a] (M^{-1} cm^{-1})	Molecular formula	MALDI-MS		t_R[b]
					Calculated	Found	
ZnPc **6a**	677	687	2.85×10^5	$C_{60}H_{33}N_8O_{12}Zn$ (MH^+)	1,121.15 $(MH)^+$	1,120.88	19.2
GaPc **6b**	680, 696	689	2.94×10^4	$C_{60}H_{32}N_8O_{12}Ga$ [$(M\text{-}OH)^+$]	1,125.14 $(M\text{-}OH)^+$	1,124.76	19.1
AlPc **6c**	677	683	3.00×10^4	$C_{60}H_{33}N_8O_{13}Al$ (M^+)	1,100.20 (M^+)	1,099.82	19.3
NiPc **6d**	673	Weak fluorescence	2.71×10^4	$C_{60}H_{32}N_8O_{12}Ni$ (M^+)	1,115.15 (M^+)	1,114.82	19.1
PdPc **6e**	665	Weak fluorescence	NM[c]	$C_{60}H_{32}N_8O_{12}Pd$ (M^+)	1,162.12 (M^+)	1,162.37	19.1
PtPc **6f**	696	Weak fluorescence	NM[c]	$C_{60}H_{32}N_8O_{12}Pt$ (M^+)	1,251.18 (M^+)	1,250.98	19.1
ZnPc **9a**	678	686	2.75×10^5	$C_{88}H_{48}N_8O_{24}Zn$ (M^+)	1,665.22 (M^+)	1,665.34	22.5
ZnPc **12**	676	689	2.67×10^5	$C_{96}H_{48}N_8O_{40}Zn$ (M^+)	2,018.13 (M^+)	2,018.50	26.1
H_2Pc **6g**	654, 675	686	3.3×10^4	$C_{60}H_{35}N_8O_{12}$ (MH^+)	1,059.24 (MH^+)	1,059.45	

The dyes were suspended in DMSO. HPLC retention times (t_R) for the MPc's using a reverse phase column and the exact mass as determined by MALDI-TOF-MS of each dye is also listed.

[a] All measurements were made at a concentration of 1×10^{-6} M. Molar absorptivities were calculated at λ_{max}.

[b] HPLC conditions: 5–95% acetonitrile/0.1 M TEAA at a flow rate of 1 ml/min.

[c] *NM* Not measured. Cannot be determined reliably due to aggregations.

J=2.1, 6.8 Hz), 7.35 (s, 2H), 7.03 (dd, 4H, *J*=2.1, 6.8 Hz), 4.33 (t, 4H, *J*=6.7 Hz, 2 CH_2O), 1.78 (m, 4H, 2 CH_2), 1.41 (m, 8H, 2 $(CH_2)_2$), 0.94 (t, 6H, 2 CH_3, *J*=7.1 Hz).

4,5-Bis(*3,5-dimethoxycarbonyl*) *phenoxyphthalonitrile* (**3**) Yield: 74%, mp 202–203°C, ^{1}H NMR (CD_3CN) δ 8.33 (t, 2H, *J*=1.45 Hz), 7.75 (d, 4H, *J*=1.45 Hz), 7.63 (s, 2H, *J*=1.45 Hz), 3.87 (s, 12 H, 4 CO_2CH_3). FAB (glycerol) 544.8 (M^+) (calculated on $C_{28}H_{20}N_2O_{10}$ 544.47).

Typical procedures are given below for the synthesis of several different MPc's. Other MPc's reported in Tables 1 and 2 were prepared by analogous protocols. NMR data was not obtainable for the following MPc's and Pc's due to the broad peaks contained in the NMR spectra.

Table 2 Absorption (λ_a) and emission (λ_e) maxima of metal free (H_2Pc) and MPc pentyl esters

Compound	Number of COOH groups	Solvent	λ_a (nm) [ε (M^{-1} cm^{-1})]	Molecular formula	MALDI-MS	
					Calculated	Found
H_2Pc **4**	4	$CHCl_3$	664 (5.67×10^4), 701 (6.50×10^4)	$C_{80}H_{74}N_8O_{12}$	1,338.54 (M^+)	1,338.30
ZnPc **5a**	4	$CHCl_3$	677	$C_{80}H_{72}N_8O_{12}Zn$	1,400.46 (M^+)	1,400.69
GaPc **5b**	4			$C_{80}H_{73}ClN_8O_{12}Ga$	1,441.43 $(M+H)^+$	1,441.22
AlPc **5c**	4			$C_{80}H_{73}ClN_8O_{12}Al$	1,399.49 $(M+H)^+$	1,399.68
NiPc **5d**	4	$CHCl_3$	670.5 (9.27×10^4)	$C_{80}H_{73}N_8O_{12}Zn$	1,395.47 $(M+H)^+$	1,395.10
PdPc (methoxy-ethyl ester) **5e**	4	Pyridine DMSO	664 (5.70×10^4) 665.5	$C_{72}H_{57}N_8O_{16}Pd$	1,395.29 $(M+H)^+$	1,394.87
H_2Pc **7**	8	$CHCl_3$	664 (1.04×10^5), 700.5 (1.21×10^5)	$C_{60}H_{32}N_8O_{12}Pt$	2,162.92 (M^+)	2,163.06
ZnPc **8a**	8	$CHCl_3$	680.5	$C_{128}H_{128}N_8O_{24}Zn$	2,224.83 (M^+)	2,225.12
GaPc **8b**	8	$CHCl_3$	697 (1.90×10^5)	$C_{128}H_{129}ClN_8O_{24}Ga$	2,268.61 $(M+H)^+$	2,268.69
H_2Pc **10**	16	$CHCl_3$	662.5 (1.47×10^5), 699.5 (1.64×10^5)	$C_{176}H_{210}N_8O_{40}$	3,077.47 (M^+)	3,077.64
ZnPc **11**	16	DMSO	643 (4.65×10^4)			

Extinction coefficients (ε) and the exact mass, as determined by MALDI-TOF-MS are also listed.

2,9,16,23-Tetrakis(4-pentyloxycarbonylhenoxy)-phthalacyanine ((**4**) 4-(4-Pentyloxycarbonylphenoxy)phthalonitrile (1.34 g, 4.0 mmol) was dissolved in anhydrous pentanol (10 ml) and heated to 65°C under argon. DBU (0.8 ml, 5.0 mmol) was added to the solution drop by drop, and the resultant mixture was refluxed for 24 h. The solvents were removed in vacuo and the residue was purified by column chromatography on silica gel eluting with hexanes/ethyl acetate mixtures (3:1). The combined fraction were evaporated to dryness and dried in vacuo to give **4** in 65% yield. MS (MALDI-TOF); calculated on $C_{80}H_{74}N_8O_{12}$ 1,338.54, found 1,338.30.

Syntheses of phthalocyanines. 2,9,16,23-tetrakis(4-carboxyphenoxy)-phthalacyanato zinc (II) (**6a**, *Scheme* 1, *path B*) A mixture of 4-(4-pentyloxycarbonylphenoxy)phthalonitrile (0.670 g, 2.0 mmol), anhydrous zinc acetate (0.183 g, 1.0 mmol) and dry pentanol (5 ml) was heated to 65°C under argon. DBU (0.4 ml, 2.5 mmol) was added dropwise to the mixture, which was subsequently refluxed for 24 h. The solvents were removed in vacuo and the residue was purified by column chromatography on silica gel using hexanes/ethyl acetate mixtures (3:1) as the eluent. The fractions were combined and the solvents were evaporated to dryness. The residue was dissolved in THF (40 ml) and added dropwise to a solution of $LiOH{\bullet}H_2O$ (1.568 g, 36.6 mmol) in 70% aqueous methanol (100 ml). The mixture was stirred at 60°C for 17 h. The organic solvents were removed in vacuo, the aqueous phase washed with chloroform (3×20 ml) and acidified to pH 2 with HCl (4 M). The resultant precipitate was centrifuged, washed with chloroform (3×20 ml) and oven dried at 60°C.

Syntheses of phthalocyanines. 2,9,16,23-tetrakis(4-carboxyphenoxy)-phthalocyanato zinc (II) (**6a,** *Scheme* 1, *path A*) A solution of 2,9,16,23-tetrakis(4-pentoxycarbonylphenoxy)phthalocyanato zinc (II) (**5a)**, 0.430 g, 0.307 mmol) in THF (40 ml) was added dropwise to a solution of $LiOH{\bullet}H_2O$ (1.568 g, 36.6 mmol) in 70% aqueous methanol (100 ml). The mixture was stirred at 60°C for 17 h. The reaction mixture work-up was done as above. MS (MALDI-TOF, anthracene) produced an isotopic cluster peak at *m*/*z* 1,120.88 (MH^+). ^{1}H NMR (DMSO-d^6) δ 9.04 (br, 4H), 8.65 (br, 4H), 8.13 (m, 8 H), 7.85 (br, 4H), 7.48 (m, 8H).

2,3,9,10,16,17,23,24-Octakis(4-pentoxycarbonyl)-phenoxyphthalocyanine (**7**, *Scheme* 2, *path A*) A mixture of 4,5-bis(4-pentoxycarbonylphenoxy)phthalonitrile (***2***, 1.08 g, 2 mmol) in dry *n*-pentanol (10 ml) was stirred at 90°C under argon and DBU (0.32 ml, 2 mmol) was added dropwise. The mixture was refluxed for 38 h. *n*-Pentanol was removed in vacuo and the crude product was purified by column chromatography (silica gel, eluent hexane/ethyl acetate 9:1 to 4:1). MS (MALDI-TOF, anthracene) yielded an isotopic cluster peak at *m*/*z* 2,164.47 (M^+).

2,3,9,10,16,17,23,24-Octakis(4-pentoxycarbonylphenoxy) phthalocyanato zinc (II) (**8a**, *path A, see Scheme* 2) A mixture of 2,3,9,10,16,17,23,24-octakis(4-pentoxycarbonylphenoxy)-phthalocyanine (**7**, 110 mg, 0.05 mmol), anhydrous zinc acetate (37 mg, 0.2 mmol) and dry DMF (10 ml) was refluxed under argon (12 h). The flask was cooled on an ice-water bath for 20 min. The mixture was poured into a beaker containing 13 g of crushed ice and the precipitate was filtered and washed with cold water, and then air dried. The crude product was purified by column chromatography (silica gel, eluent: hexane/ethyl acetate, 4:1 to 3:1). MS (MALDI-TOF, anthracene) yielded an isotopic cluster peak at *m*/*z* 2,227.84 (M^+).

Synthesis of zinc phthalocyanine N, hydroxysuccinimide ester The synthesis of NHS ester derivatives of carboxylate zinc-Pc **6a** was adapted from a published procedure and will only be described briefly here [27]. A solution of carboxylate Pc **6a** was dissolved in dry DMF and added to a solution of NHS and DCC (1.5 equiv. each) in dry DMF. The reaction was carried out at room temperature under agitation and allowed to react overnight. The reaction was then pooled and the product was precipitated by the addition of diethyl ether, isolated by centrifugation and dried under vacuum for several hours.

UV/Vis spectra Absorption spectra were collected on an Ultrospec 4000 single beam UV/visible spectrophotometer (Amersham Biosciences, Piscataway, NJ) with 1 cm quartz cuvettes using Swift software (Amersham Biosciences). The concentrations of the MPc dyes used in these measurements were $1–100\times10^{-6}$ M to minimize the formation of aggregates [28]. The molar absorptivity was calculated from a least squares fit of the absorbance versus concentration for each dye. An absorption spectrum of the reference solvent, which was DMSO, was obtained and subtracted prior to the acquisition of each spectrum.

Fluorescence measurements Steady-state fluorescence spectra were acquired using a Spex Fluorolog-3 equipped with a 450 W Xenon light source (Horiba Jobin Yvon, Edison, NJ) and a Hamamatsu R928 photomultiplier tube (Bridgewater, NJ). DM300 software was used for data analysis. Fluorescence spectra were obtained using an excitation wavelength of 680 nm for Pc and MPc dyes with a bandpass of 2 nm for both the excitation and emission monochromators.

The quantum yields were determined relative to a secondary standard using the equation [29, 30];

$$\Phi_{f(x)} = \left(A_{standard}/A_{sample}\right)\left(F_{sample}/F_{standard}\right) \times \left(n_{sample}/n_{standard}\right)^2 \Phi_{standard} \quad (1)$$

where F_{sample} and $F_{standard}$ are the measured fluorescence for the sample and standard, respectively, $A_{standard}$ and A_{sample} are the measured absorbance, n_{sample} and $n_{standard}$ are the refractive index of the solvent used for the sample and standard, respectively, and $\Phi_{standard}$ is the quantum yield of the secondary standard. The secondary standard used in these experiments was diethyloxatricarbocyanine iodide (DOTCI). The quantum yield of DOTCI has been reported to be 0.63 in DMSO [31]. For the determination of the quantum yields, the secondary standard was excited at 680 nm to avoid post correction analysis. To minimize any error due to reabsorption or aggregation, all measurements were made with highly dilute solutions having an absorbance between 0.04 and 0.05 for a 1 cm path length.

Time-resolved fluorescence measurements Time-resolved fluorescence decays were collected using time-correlated single photon counting (TCSPC) acquired on a Fluotime 200 instrument (Picoquant, Berlin, Germany). The excitation source was a 680 nm pulsed diode laser (PDL 800, Picoquant). Since rotational diffusion could lead to distortion of the fluorescence decay, a polarizer was inserted into the system and set at the magic angle of 54.7°. The spectrometer consisted of a monochromator (ScienceTech 9030) and a photomultiplier tube (PMS 182-M single photon detection). All electronics for TCSPC were situated on a single PC card resident on the bus of the PC and consisted of a constant fraction discriminator and time-to-digital converter with an instrument response function of ~450 ps (FWHM). Time-resolved data were analyzed using FluoFit software (Picoquant, Berlin, Germany). The fluorescence decays were collected until ~10,000 counts were accumulated in the time channel with the most counts and fit to single or multi-exponential function by an iterative reconvolution algorithm using nonlinear least squares. The instrument response function was always collected to the same maximum number of counts as the fluorescence decay data. The quality of the fit was determined by the randomness of the weighted residuals and the value of χ^2.

Photobleaching measurements Bleaching curves were recorded by continuously irradiating several MPc's, a dicarbocyanine (IRD700) and tricarbocyanine (DOTCI) using a 680 nm diode laser (Picoquant, Berlin, Germany) as the excitation source. The beam waist was measured by mounting a razor blade on a translation stage and measuring the beam power using a laser power meter. The product of $I_0\sigma$ (laser intensity in photons s^{-1} $cm^{-2}\times$ absorption cross section in cm^2), which provides the electronic absorption rate, k_a, was kept constant for all samples. The absorption cross-section, σ, was determined by multiplying 3.8×10^{-21} by the molar extinction coefficient, ε. The dyes were dissolved in DMSO at a concentration of 1.0 μM and were not degassed. A linear least squares fit to a semi-log plot of time versus the fluorescence intensity was used to calculate the photobleaching lifetime, τ_b. The quantum yield of photobleaching, Φ_d, was determined from the following equation;

$$\tau_b = \frac{1}{k_a \Phi_d} \quad (2)$$

An estimation of the photon yield per molecule was calculated from the ratio of the fluorescence quantum yield to the photo-destruction quantum yield.

Labeling of streptavidin with ZnPc **6a, 12** *active ester* Conjugation of ZnPc **6a** or **12** to streptavidin was performed in 0.1 M HEPES buffer, pH 8, using a streptavidin concentration of 10 μM. A solution of *N*-hydroxysuccinimide tetraester of ZnPc **6a** or **12** in DMSO was added to the streptavidin solution to achieve the desired dye-to-protein molar concentration ratio of 10:1. The reaction was incubated at room temperature for 24 h followed by analysis and purification using reverse-phase HPLC. Separation of the products was performed on a C18 column using a linear gradient of 30–75% acetonitrile/0.1TEAA for 30 min at a flow rate of 1 ml/min. The elution of the conjugates was monitored using fluorescence detection at 686 nm for excitation and 693 nm for emission.

Results

Synthesis of metal and metal-free phthalocyanines (*MPc and Pc*) Schemes 1–3 describe the methods used to prepare tetra-, octa-, and hexadeca-carboxylate Pc's and MPc's. The metal-free analogues, which can serve as precursors for various MPc's, are usually prepared by base-promoted cyclization of phthalonitriles. For the synthesis of MPc's one can imagine two routes: one through the introduction of the central metal into the metal-free Pc (path A in Schemes 1–3) or direct metal templated MPc preparation (path B in Schemes 1–3).

The starting substituted phthalonitriles **1**–**3** were prepared from 4-nitrophthalonitrile or 4,5-dichlorophthalonitrile and appropriate phenols according to literature protocols [5, 32, 33]. Synthesis of the previously reported

Zn-tetracarboxylate Pc **6a** started with phthalonitrile **1** as the pentyl ester [34, 35]. Refluxing of **1** in pentanol in the absence of a metal salt (Scheme 1, path A) gave the metal-free, tetra-ester Pc **4**. Refluxing of **4** in DMF in the presence of an excess (>10 equiv.) of $Zn(OAc)_2$ converted it to the ZnPc tetra-pentyl ester **5a**. The preparation of this compound was more directly accomplished by refluxing of phthalonitrile **1** in pentanol in the presence of DBU and $Zn(OAc)_2$ (Scheme 1, path B). This direct synthetic route also worked well for the preparation of Ni, Pd and Pt MPc's as tetra-pentyl esters **5d**–**5f**. Because path B consisted of one less step than path A, the overall yields of the compounds prepared by this method were higher than those for path A. Moreover, the cyclization itself was facilitated in the presence of the metal giving higher yields for the synthesis of MPc's than for metal-free Pc's.

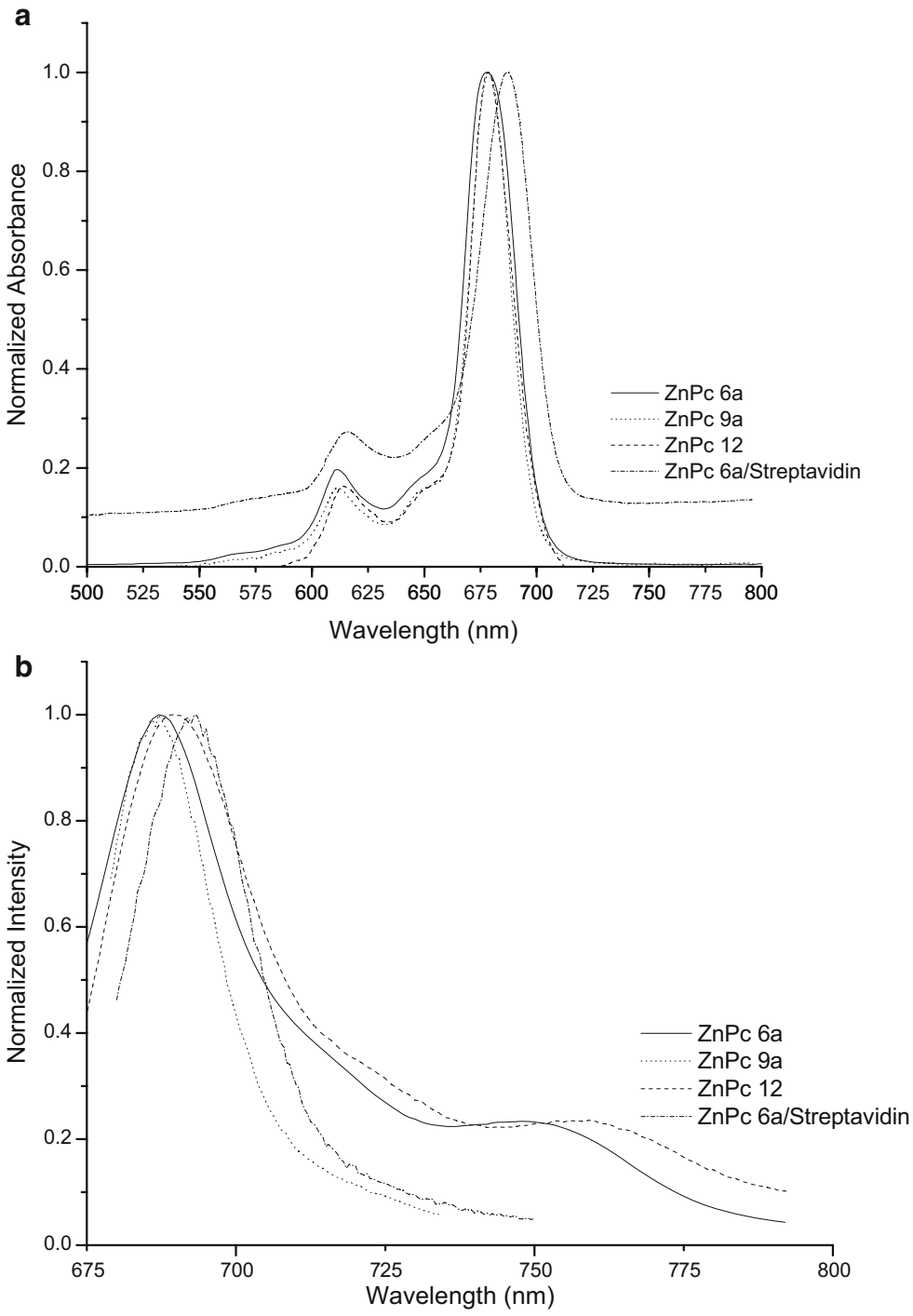

Fig. 1 Absorption (**a**) and emission (**b**) spectra of ZnPc dyes along with the ZnPc **6a**/streptavidin complex. The emission spectra were obtained at an excitation wavelength of 675 nm. The emission spectra were normalized to the maxima. All emission spectra were collected in DMSO at a concentration of ~1.0 μM, while the absorption spectra used dye concentrations that varied from 1–100 μM

For group IIIa MPc's, direct synthesis of tetracarboxylates GaPc **6b** and AlPc **6c** by refluxing the substituted phthalonitrile and the appropriate metal salt in *n*-pentanol in an inert atmosphere with the subsequent hydrolysis of MPc's esters **5b** and **5c** failed. Thus, only Path B was available for the synthesis of these derivatives, which consists in the reaction of metal free Pc (tetra-ester) **4** refluxed with $GaCl_3$ or $AlCl_3$ to give metallated Pc's esters **5b** and **5c**, correspondingly.

The methyl ester of phthalonitrile **1** worked well for either path A or path B, but gave mixtures of esters in the resulting Pc (or MPc) ester products, complicating their purification. In order to avoid such complications, we matched the ester group to the preferred alcohol. Pentanol gave the most flexibility in terms of temperature range for the reaction and thus, the pentyl ester of starting phthalonitriles (**1**–**3**) became our standard.

To generate either the metal-free Pc or MPc tetracarboxylates, their pentyl esters are saponified with LiOH in a tertiary mixture of water, THF and methanol. Both the MPc esters and the lithium salts generally stay soluble in this medium and upon acidification with aqueous HCl, the pure free acids are readily obtained in quantitative yields. Purification of these compounds can be accomplished by washing the precipitate with chloroform and dissolving the solid in aqueous hydroxide solution and re-precipitating the free acid (Pc or MPc) into aqueous acid (HCl). Alternatively, a DMF solution of the free acid can be precipitated into an excess of diethyl ether.

Because the central atom of the group IIIa MPc's is trivalent, the MPc's should have axial ligands. According to the MALDI data, the ligand of Ga and Al MPc's (esters) is chloride (see Table 2). Under the subsequent hydrolysis reaction conditions, chloride was substituted by a hydroxyl group. This transformation was seen in the MALDI analysis of tetracarboxylate AlPc **6c**, where the molecular ion $C_{60}H_{33}N_8O_{13}Al$ was observed. The corresponding GaPc **6b** did not exhibit molecular peaks in MALDI-TOF as only $(M\text{-}OH)^+$ peaks were observed. Despite the absence of mass spectral evidence for the hydroxyl ligand on the GaPc **6b**, we assumed its presence in analogy with AlPc **6c** and its requirement for filling of the Ga valencies.

For the synthesis of the octa and hexadeca substituted MPc's **9** and **12** (see Scheme 2 and 3, respectively), we used the same synthetic routes. It was possible to use both paths A and B, but again the use of path B gave higher yields. Phthalonitriles **2** and **3** used in the syntheses of MPc's esters **8** and **11**, were more sterically hindered and having different aromatic electron density because of substitution, so their cyclization reaction gave lower yields of Pc's and MPc's. Increasing the reaction temperature did not increase the yields of the final compounds. The rate of hydrolysis of pentyl esters of such MPc's **8** and **11** was slower and required up to 5 times higher concentrations of the hydroxide to achieve complete saponification.

Spectral properties Absorption spectra of Pc dyes typically have two main bands, one in the UV and another in the near-IR. The higher energy band (~350 nm) is known as the B or Soret band [17, 36]. The lower energy band, typically appearing around 680 nm, is often referred to as the Q-band. The Q-band exhibits vibronic structure in solution between 610 and 640 nm [17, 37, 38].

The absorption and fluorescence emission properties, including the molar absorptivities for the Pc and MPc's containing various degrees of carboxylation are listed in Table 1. The absorption and emission spectra of the ZnPc dyes with different degrees of carboxylation are shown in Fig. 1a and b, respectively. Tetracarboxylate ZnPc **6a** shows a single absorption peak at 677 nm with a blue-shifted band at 610 nm. Upon excitation at 675 nm, **6a** exhibited strong fluorescence with a maximum at 687 nm and a shoulder at 759 nm. The absorption and emission spectra for octa- and hexadecacarboxylate ZnPc **9a** and **12** in DMSO were similar to those exhibited by tetracarboxylate ZnPc **6a**. However, the emission shoulder appearing at ~759 nm for **6a** and **12** was absent in the case of **9a**. The absorption and emission spectra of the following tetracarboxylates—metal free Pc **6g**, GaPc **6b** and AlPc **6c** —in DMSO are shown in Fig. 2a and b, respectively. GaPc **6b** exhibited a split in its Q-band with absorption maxima at 680 and 696 nm, while AlPc **6c** showed only a singlet Q-band with an absorption maximum at 677 nm. In the case of metal free Pc **6g**, a very broad absorption spectrum was observed with a Q-band split showing a maximum at 675 nm. GaPc **6b**, AlPc **6c** and metal free Pc **6g** showed emission maxima that ranged between 683 and 689 nm with a slight red-shift seen for the maxima in the series, Al, H_2 and Ga. The absorption maxima, extinction coefficients and MALDI-MS data for the MPc esters **5**, **8** and **11** are also listed in Table 2. The absorption characteristics are consistent with the data seen for the free acids. In addition, the calculated mass agreed favorably to that obtained from the MALDI-MS, indicating the assigned molecular structure of the dye was correct.

The absorption spectra of tetra-, octa- and hexadecacarboxylate ZnPc **6a**, **9a** and **12**, tetracarboxylate AlPc **6c** and GaPc **6b** in HEPES at pH 8 are illustrated in Fig. 3. The absorbance spectra for these compounds were also measured in CAPS buffer at pH 11 and the results were similar to those shown in Fig. 3 for HEPES buffer. Most of these compounds showed similar absorption maxima, but broader absorption envelopes compared to the same spectra in DMSO with the absorption maximum slightly blue-shifted (~645 nm in HEPES compared to ~675 nm in DMSO). However, **9a** and **12** showed absorption characteristics in

both HEPES and CAPS buffer that were very similar to those observed in DMSO, both in terms of the spectral widths and absorption maxima.

Photophysics The fluorescence quantum yields of the MPc complexes were measured with respect to a secondary standard, diethyloxatricarbocyanine iodide (DOTCI), in DMSO, which has a documented quantum yield of 0.63 [31]. The quantum yields for ZnPc **6a**, **9a** and **12** with different degrees of carboxylation ranged from 0.40–0.41, while the quantum yields for GaPc **6b** and AlPc **6c** were 0.58 and 0.60, respectively. The quantum yields were also

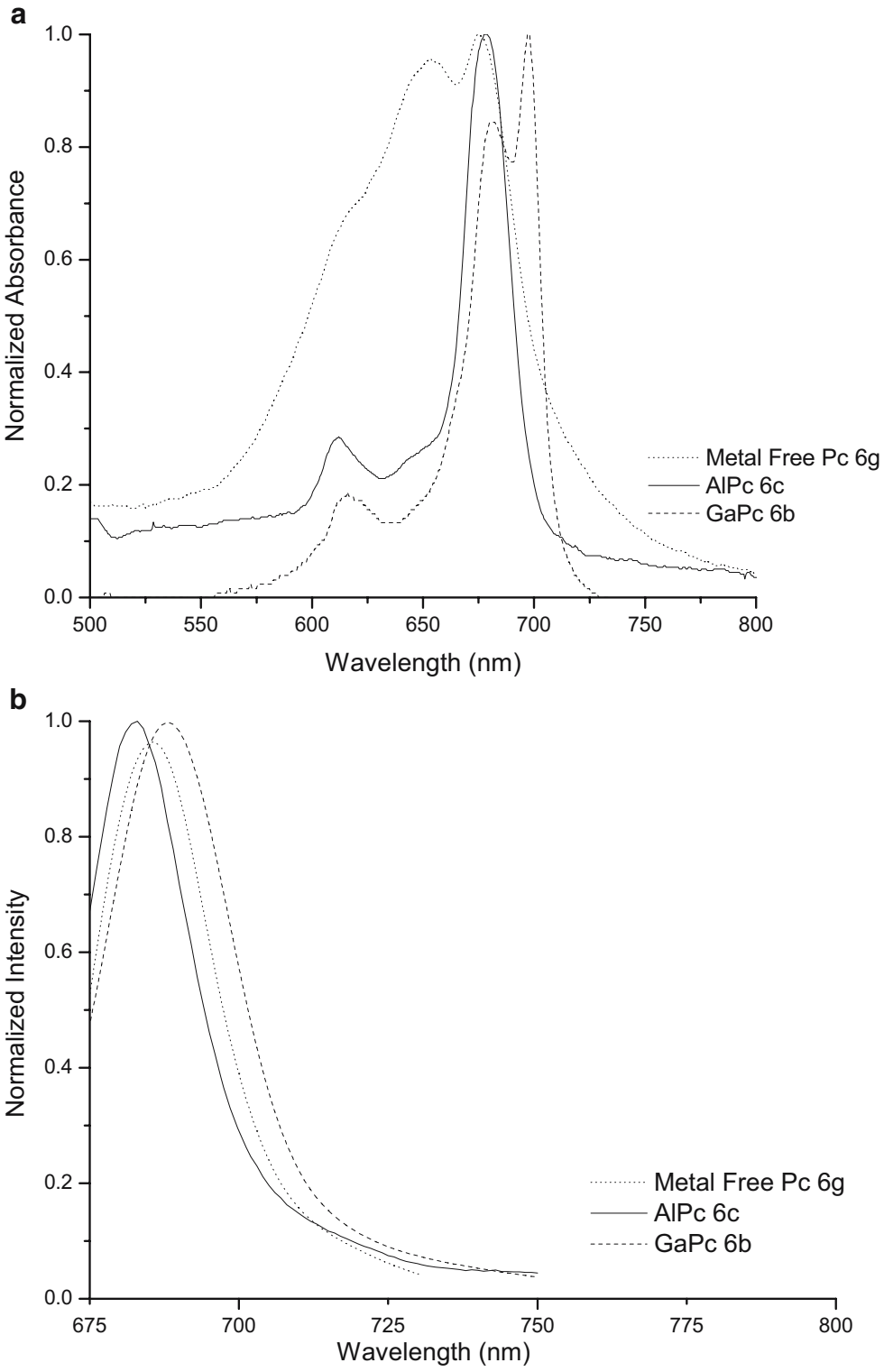

Fig. 2 Normalized absorption (**a**) and emission (**b**) spectra for a metal free Pc and several metal substituted Pc dyes (Zn, Al, Ga) dissolved in DMSO. The emission spectra were excited at the absorption maximum for each dye at a concentration of 1.0 μM. In all cases, the tetracarboxylated dyes were used in these measurements

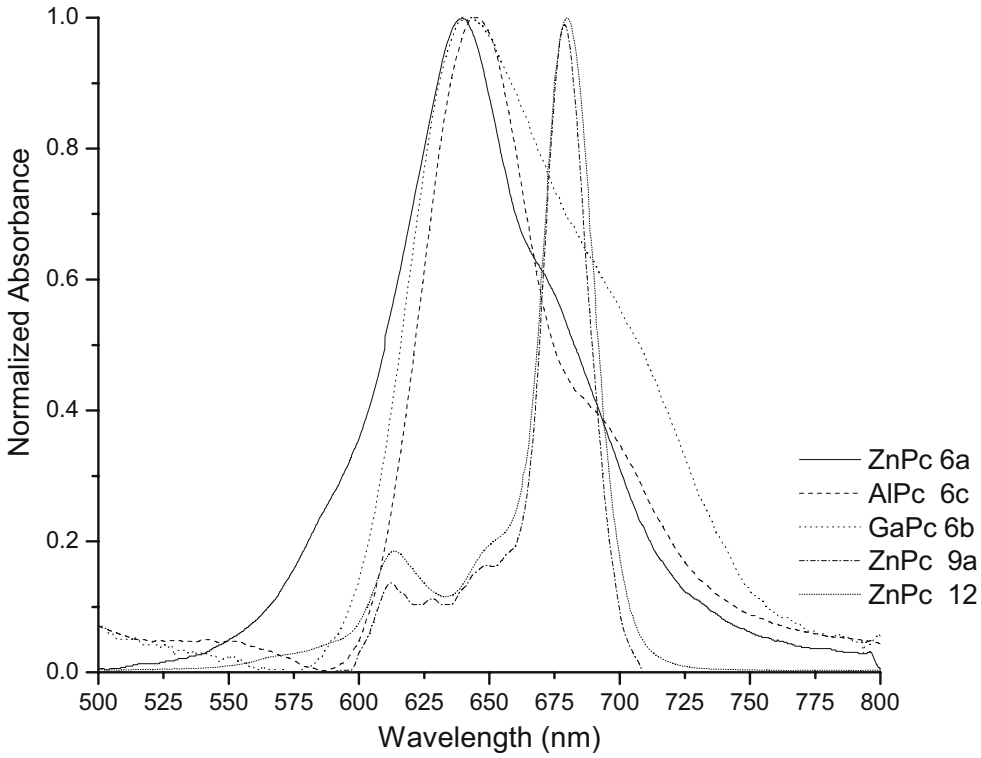

Fig. 3 Absorption spectrum for MPc's in HEPES buffer, pH 8. The concentrations of dyes used in these measurements were 1.0×10^{-6} M. The absorption spectra were normalized with respect to the absorption maxima

determined for the MPc's in CAPS buffer at pH 11 with the result shown in Table 3. The quantum yields for the ZnPc's **6a**, **9a** and **12** and GaPc **6b** ranged from 0.11–0.14, whereas the quantum yield for AlPc **6c** was determined to be 0.31. The radiative decay rates for several of the MPc's were estimated using the emission and extinction profiles and the Strickler–Berg equation [39], which yielded rates calculated for ZnPc **6a**, GaPc **6b** and AlPc **6c** of $0.64\times10^{9}s^{-1}$, 0.58×10^{9} s^{-1}, and 0.48×10^{9} s^{-1}, respectively (see Table 3).

The fluorescence lifetimes for each MPc dye are given in Table 3 as well. ZnPc **6a** had a lifetime of 3.1 ns with its decay kinetics adequately described by a single exponential function. AlPc **6c** was best fit to a double exponential function yielding fluorescence lifetimes of 5.0 and 0.64 ns. In addition, GaPc **6b** exhibited a multi-exponential decay with the longest lifetime being 3.5 ns. Octacarboxylate ZnPc **9a** was best fit to a monoexponential function with a lifetime of 2.9 ns while hexadecacarboxylate ZnPc **12** displayed a lifetime of 2.8 ns (see Table 2).

Table 3 Fluorescence lifetimes (τ_f), fluorescence quantum yields (Φ_f), photobleaching quantum yields (Φ_d), and photon yields per molecule (n_f) for the standard, DOTCI, metal free and several metal Pc dyes

Compound	τ_f (ns)	τ_2 (ns)	Φ_f	Φ_f CAPS	Φ_d	n_f	k_r ($\times10^9$ s^{-1})	χ^2
ZnPc **6a**	3.1		0.41	0.11	5.0×10^{-7}	1.3×10^{6}	0.64	1.43
ZnPc **9a**	2.9		0.40	0.11	4.3×10^{-7}	1.4×10^{6}		1.49
ZnPc **12**	2.8		0.40	0.12	1.3×10^{-7}	5.0×10^{6}		1.27
GaPc **6b**	3.5	0.57	0.58	0.14	2.3×10^{-6}	2.7×10^{5}	0.58	1.48
AlPc **6c**	5.0	0.64	0.60	0.31	2.8×10^{-5}	2.1×10^{4}	0.48	1.09
DOTCI	nd[a]	nd[a]	0.63		7.0×10^{-3}	90.0		
IRDye 700	nd[a]	nd[a]	0.70		4.6×10^{-6}	1.5×10^{5}		
ZnPc **6a**/streptavidin	2.85			0.16				

Radiative rates were calculated using the Strickler–Berg relationship. Samples were prepared to have an optical density of ≤0.05 at the λ_{max}. The χ^2 value for each decay profile is also presented. All of these photophysical properties were measured in DMSO, except for the fluorescence quantum yields measured in CAPS (pH=11.0) and the ZnPc **6a**/streptavidin conjugate, which was measured in HEPES buffer (pH=8.0).
[a] The fluorescence lifetimes for DOTCI and IRD700 were not determined (*nd*).

The photodestruction quantum yields along with the photon yields per molecule for tetra-, octa- and hexadeca-carboxylate ZnPc **6a**, **9a** and **12**, as well as AlPc **6c** and GaPc **6b** are listed in Table 3. The results indicate decreased photostability for AlPc **6c** compared to ZnPc **6a** with a photobleaching quantum yield of 2.8×10^{-5} for AlPc and 5.0×10^{-7} for ZnPc. For the ZnPc's **6a**, **9a** and **12**, increasing the degree of carboxylation provided dyes with increased photostabilities and consequently, improved photon yields on a per molecule basis. A qualitative examination of the photobleaching data showed that these ZnPc dyes were significantly more photostable than a commercially available tricarbocyanine dye (see Fig. 4).

The photophysical and spectral properties were also investigated when tetracarboxylate ZnPc **6a** was covalently attached to streptavidin, a 55 kDa protein. Results indicated a slight shift in the absorption and emission maxima for the conjugate compared to the dye with the absorption maxima appearing at 687 nm and the emission maxima at 693 nm (see Fig. 1a and b). In addition, the fluorescence lifetime of the conjugate was found to be 2.85 ns, slightly shorter than that seen for the ZnPc dye.

Evaluation of the ZnPc-streptavidin conjugation mixture of ZnPc **6a** and **12** were analyzed using reverse-phase chromatography with fluorescence detection to monitor both the conjugate and free ZnPc dye. The chromatograms for the reaction mixtures of ZnPc **6a** only and streptavidin conjugated to **6a** or **12** are shown in Fig. 5a and b. As can be seen, the free dye peak is visible in the ZnPc/streptavidin reaction because the dye was available at a tenfold molar excess compared to the protein. Also, the chromatogram demonstrated the presence of multiple peaks that were not present for the reaction mixture containing no streptavidin, indicating that streptavidin molecules are multiply labeled with ZnPc **6a** or **12**.

Discussion

Modeling and experimental evaluation of the electronic properties of Pc's and MPc's have been reported [40–42]. As a starting point, Gouterman's model provides useful background in predicting the origin of the main spectral features of metal and metal free Pc's in terms of four orbitals, HOMO-1, HOMO, LUMO, and LUMO+1 [43, 44]. The Q band is assigned to the a_{1u} (π) to e_g (π^*) transition, while the B band is assigned to an a_{2u} (π) to e_g (π^*) transition. In Pc's, the 1_{a1u} and 1_{a2u} orbitals become widely separated in energy resulting from the presence of the aza bridges and consequently, the Q and B bands appear at approximately 680 and 350 nm, respectively [45, 46]. For metal free Pc's, Q-band splitting is indicative of D_{2h} symmetry with the orbital degeneracy lifted, while the

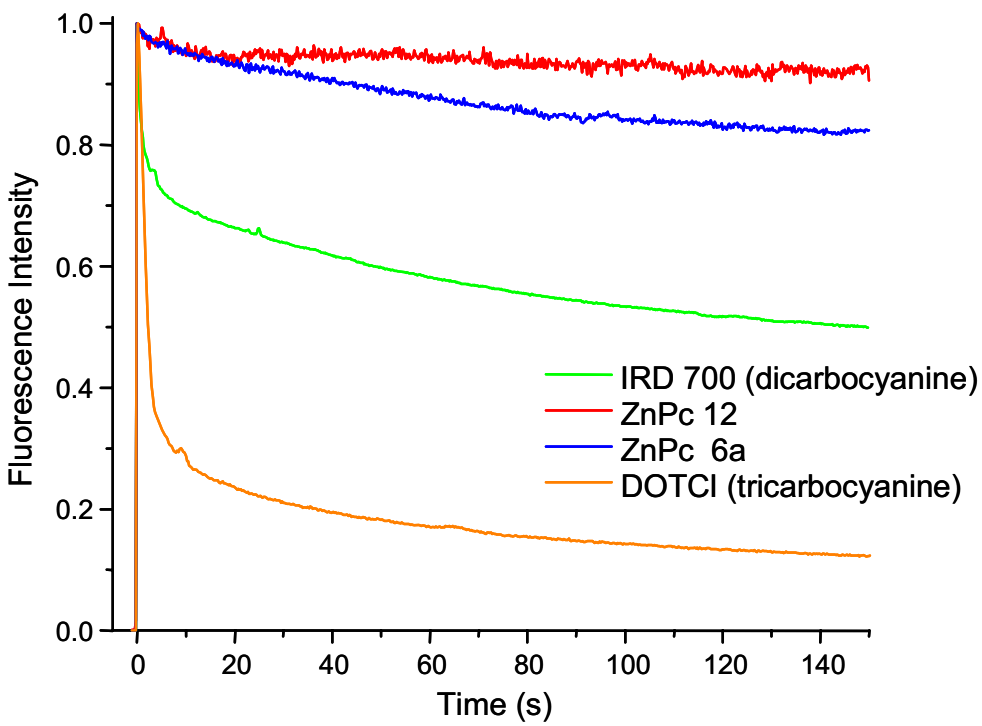

Fig. 4 Photobleaching profiles for several ZnPc dyes, IRD700, and DOTCI. The photobleaching decay profiles were collected using 680 excitation by constantly irradiating a 1.0 μM solution and continuously monitoring the fluorescence emission

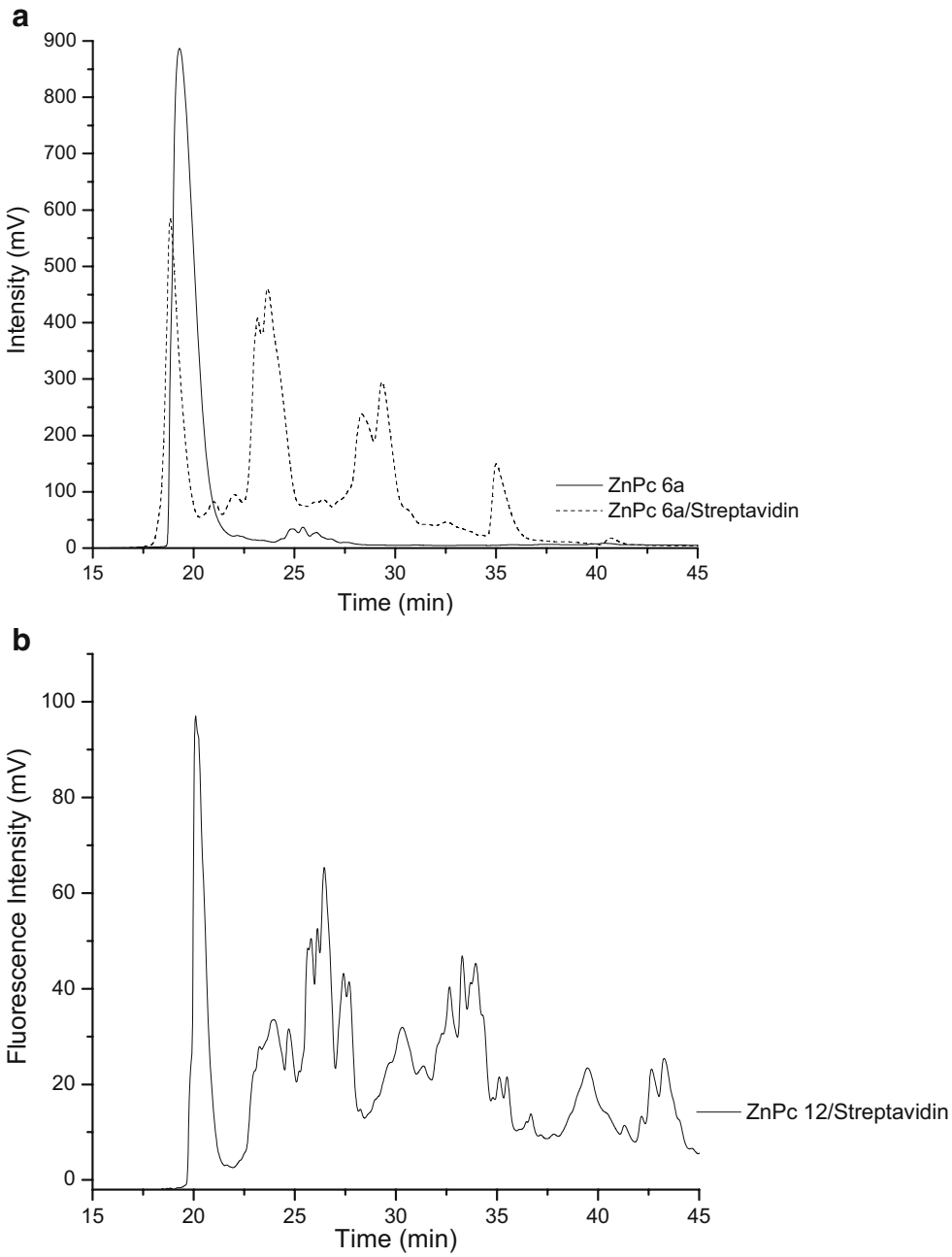

Fig. 5 Chromatogram showing the elution of (**a**) ZnPc 6a by itself (t_r=19.2 min) and ZnPc **6a**/streptavidin conjugate (t_r=23.1, 28.5 and 35.0 min). (**b**) Chromatogram showing the conjugation reaction of ZnPc 12 with streptavidin. The fluorescence detector was set at λ_{ex}=686 nm and λ_{em}=693 nm. See experimental section for an explanation of the chromatographic conditions

symmetry of MPc's is generally D_{4h} [47]. Depending on the size of the metal ion, accommodation of the metal can result in doming or ring expansion in the macrocycle causing the symmetry of the molecule to become distorted [48], inducing electronic perturbations that are manifested by bathochromic shifts in the absorption bands and/or Q-band splitting. Significant mixing of the transition metal d-orbitals and the π orbitals of the macrocycle produce changes in the electronic features of the MPc's as well with the extent of interaction dependent upon the nature of the central metal. The metal-macrocycle interaction have been analyzed in detail by Rosa and Baerends [49].

For the MPc's investigated in this paper, the absorption spectra for tetra-, octa- and hexadecacarboxylate ZnPc **6a**, **9a** and **12** and tetracarboxylate AlPc **6c** are typical for MPc compounds exhibiting a sharp and narrow Q band suggesting monomeric species and a higher energy Soret band when placed in DMSO solvents (see Figs. 1 and 2). In addition, they showed an additional shoulder to the blue of the Q-band, which can be attributed to combination

overtones of Q-band electronic transitions [49]. For GaPc, it has been reported that the Ga center is approximately 0.45 Å out of plane; the Q-band split observed in this study suggested that doming did occur in this MPc causing a split in the orbital degeneracy due to symmetry changes [50]. The absorption spectrum with a split in the Q-band for metal free Pc **6g** is also consistent with D_{2h} symmetry.

Pc complexes with a light closed-shell central metal ion are typically highly fluorescent [19]. The fluorescence emission of the Pc's studied in this report in DMSO have strong emission peaks around 687 nm with the emission profile for tetracarboxylate ZnPc **6a** showing a small shoulder around 750 nm, which may indicate ligand-to-metal charge transfer. Excitation at 696 nm for GaPc **6b** resulted in no detectable fluorescence, suggesting vibronic splitting of the S_1 electronic state. The NiPc **6d**, PdPc **6e** and PtPc **6f** showed weak fluorescence (see Table 1) due to these metals larger atomic numbers compared to the Zn, Al, and Ga metal centers, resulting in higher rates of intersystem crossing from spin orbit coupling artifacts.

For many MPc compounds, self-association occurs readily in aqueous solutions due to intermolecular association with the degree of association dependent upon the identity of the metal ion and the peripheral substitutions on the benzo groups [17, 51]. For example, introduction of substituents in the 1,3 positions produces a shift to the red as opposed to substituents placed at the 1,4 positions. Aggregation effects of several Pc dyes have been documented [52, 53]. Two main aggregate species have been identified as J and H aggregates with J-aggregates marked by a red-shift in the monomer peak due to head-to-tail aggregation, while H-aggregates correspond to face-to-face dimerization marked by a blue shift [54, 55]. The absorption spectra for ZnPc **6a** in HEPES buffer at pH 8 (see Fig. 3) exhibited extensive broadening of the Q band with a blue shift in the absorption maximum indicative of H-aggregate formation. In addition, AlPc **6c** and GaPc **6b** showed the same artifacts in their absorption profiles collected in HEPES buffer. However, as the degree of carboxylation increased, the absorbance spectra more resembled those in DMSO, where aggregation effects were expected to be minimal. For example, octa- and hexadeca-carboxylate ZnPc **9a** and **12** showed narrow absorption envelopes with the absorption maximum very similar to that seen in DMSO. Therefore, high degrees of carboxylation (>4 carboxylate groups) seem to be fairly effective in minimizing ground state aggregation for ZnPc dyes. Interestingly, tetracarboxylate ZnPc **6a** in CAPS buffer (pH=11.0) showed a narrower absorption profile compared to this same compound in HEPES, suggesting a smaller propensity to aggregate at higher pH, which could be ascribed to a higher population of deprotonated species at higher pH values.

The trends observed in the quantum yields for each MPc in DMSO can be explained in terms of heavy atom effects [19, 46]. As the atomic number of the heavy atom, which in this case is the metal center, increases one would expect the quantum yield to decrease due to increases in the intersystem crossing rate resulting from heavy-atom induced spin-orbit coupling. For the data collected herein, the quantum yields for Zn, Ga, and Al did show an increase as the atomic number decreased for this series. Indeed, previous reports on MPc's have indicated that Al-analogs typically show relatively larger quantum yields compared to other MPc's due to its smaller atomic number [56]. Inspection of the data in Table 3 also indicated that the degree of carboxylation added to the ZnPc macrocycle did not significantly affect the fluorescence quantum yields for this series of dyes when in DMSO.

In HEPES (pH=8.0), the quantum yields for the MPc compounds studied herein were observed to be less than 1% (data not shown). However, when the buffer pH was increased (CAPS, pH=11.0) the fluorescence quantum yields for all of these dyes improved dramatically [57]. The fluorescence quantum yield for the ZnPc **6a**/streptavidin conjugate was also found to be significantly higher compared to the free dye only in HEPES buffer. If we assume that the quantum yields for the ground state aggregated forms of these dyes are negligible compared to their monomeric counterparts, the relatively small quantum yields seen for these dyes in HEPES buffer is most likely due to a lower ground state population of the monomeric form. While differences in extinction should correct for this population difference, the broad absorption profiles associated with the aggregates produced an apparent extinction coefficient that did not correct for the lower number of monomeric species (see Eq. 1).

The fluorescence lifetimes for the MPc's showed the same trend as that seen for the fluorescence quantum yields, with the lifetime of AlPc **6c** significantly longer than that of ZnPc **6a** and GaPc **6b**, which have larger atomic numbers compared to Al and thus, would be expected to show shorter fluorescence lifetimes based on heavy-atom mediated effects. As can also be noticed in the data displayed in Table 3, the fluorescence lifetimes were generally independent of the number of substituents added to the periphery of the ZnPc dyes. The identity of the short-lived component observed for Al and Ga is uncertain.

The nature of MPc intermolecular interactions intimately affects the photostability of MPc's and plays a central role in determining the number of photons generated per molecule, a key parameter in a number of ultra-sensitive fluorescence measurements and imaging as well [17]. Among the MPc's investigated in this work, tetracarboxylate AlPc **6c** was nearly 2 orders of magnitude less photochemically stable compared to the same tetracarboxylate ZnPc **6a**

and one order of magnitude less stable than GaPc **6b**. Interestingly, the photodestruction quantum yields for tetra-, octa- and hexadecacarboxylate ZnPc **6a**, **9a** and **12** showed increased photostability with higher degrees of carboxylation. It is clear that a high degree of carboxylation mitigates intermolecular interactions resulting in enhanced photostabilities. The photobleaching quantum yields reported in Table 3 illustrate the superiority of the Pc dyes compared to their cyanine counterparts as these dyes are less photochemically stable and thus, provide fewer photons on a per molecule basis. A detailed investigation of the photostability of several metal phthalocyanines has been discussed previously [58]. The authors examined factors that influenced the photobleaching process suggesting that photobleaching was related to the change in the electronic distribution of the molecular structure influenced by the identity of the metal center.

The carboxylic groups not only provided a means for improving the water compatibility of the Pc dyes investigated herein, but could serve the dual function of allowing for their chemical modification by reacting the peripheral carboxylate groups with N-hydroxysuccinimide and DCC to form an activated ester for the covalent binding of targets bearing primary amine groups, such as streptavidin. Inspection of the spectral properties of the ZnPc **6a**/streptavidin complex indicated a slight bathochromic shift in its absorption maximum compared to the free dye in DMSO as well as a slight red-shift in its emission maximum. The dye-to-protein concentration ratio was set to 10:1 in order to minimize multiple streptavidin molecules strapped to single **6a** or **12** molecules due to the 4 or 16 active sites around the periphery of the dye. However, there was still the appearance of several peaks within the chromatographic trace (see Fig. 5a) besides the free dye and single dye/protein conjugate peak indicating the existence of multiple streptavidins attached to the dye or multiple dye molecules attached to a single streptavidin. While hexadecacarboxylate ZnPc **12** could be viewed as a better labeling fluor due to its improved water compatibility and photochemical stability, the presence of spurious conjugate peaks in the chromatogram (see Fig. 5b) besides the 1:1 complex, would make purification and quantification difficult. While we are uncertain of the identity of these spurious peaks, an LC–MS analysis could provide information as to the identity of the multiple peaks contained in this chromatogram.

Conclusions

This work presented facile routes for the preparation of heavily carboxylated MPc-type dyes and also, the photophysical and spectral properties of several metal free and MPc derivatives and the effects of the metal and ring substituents on these properties. In general, the MPc dyes exhibited higher photostability compared to other commercially available fluorophores used for near-IR applications, which will have important ramifications in ultra-sensitive measurements as well as imaging. The fluorescence quantum yields and lifetimes were found to depend on the metal substituent, but not on the degree of carboxylation.

The challenge with the use of MPc-based dyes is their poor compatibility with aqueous solvents due to their high propensity to undergo self-aggregation. However, aggregation artifacts could be mitigated through modification of the periphery of the macrocycle by appending large numbers of polar/ionic groups that inhibit dye–dye interactions. For the dyes investigated here, incorporating carboxylic acid groups proved to be an effective approach for minimizing ground state aggregation as observed from the spectral properties of octa- and hexadecacarboxylate ZnPc's **9a** and **12** in buffered media. Interestingly, high degrees of carboxylation also provided better photochemical stabilities. The initial results obtained for the conjugation studies has prompted future work to focus on the optimization of labeling conditions with various ZnPc dyes, especially those that are heavily carboxylated to provide high quantum yield and photostable conjugates that can be easily purified.

Acknowledgments This work has been supported by the National Institutes of Health (HG-01499, CA-099246), the National Science Foundation (EPS-0346411, CHE-0304833) and the Louisiana Board of Regents. The authors would also like to thank Dr. Maverick for his help and insightful discussions.

References

1. Bryant GC, Cook MJ, Ryan TG, Thorne AJ (1995) Liquid-crystalline polymeric phthalocyanines. J Chem Soc Chem Commun 4:467–468
2. Piechocki C, Simon J, Skoulios A, Guillon D, Weber P (1982) Discotic mesophases obtained from substituted metallophthalocyanines—toward liquid-crystalline one-dimensional conductors. J Am Chem Soc 104(19):5245–5247
3. Tedesco AC (2003) Synthesis, photophysical and photochemical aspects of phthalocyanines for photodynamic therapy. Curr Org Chem 7:187–196
4. Margaron P, Gregoire MJ, Scasnar V, Ali H, van Lier JE (1996) Structure-photodynamic activity relationships of a series of 4-substituted zinc phthalocyanines. Photochem Photobiol 63(2): 217–223
5. Liu W, Jensen TJ, Fronczek FR, Hammer RP, Smith KM, Vicente MGH (2005) Synthesis and cellular studies of nonaggregated water-soluble phthalocyanines. J Med Chem 48(4):1033–1041
6. Gopel W (1991) Phthalocyanine prototype interfaces—their importance for designing chemical sensor and molecular electronic devices. Synth Met 41(3):1087–1093
7. Zhou R, Josse F, Gopel W, Ozturk ZZ, Bekaroglu O (1996) Phthalocyanines as sensitive materials for chemical sensors. Appl Organomet Chem 10(8):557–577

8. Langlois R, Ali H, Brasseur N, Wagner JR, Vanlier JE (1986) Biological-activities of phthalocyanines 0.4. Type-Ii sensitized photooxidation of L-tryptophan and cholesterol by sulfonated metallo phthalocyanines. Photochem Photobiol 44(2):117–123
9. Hu M, Brasseur N, Yildiz SZ, van Lier JE, Leznoff CC (1998) Hydroxyphthalocyanines as potential photodynamic agents for cancer therapy. J Med Chem 41(11):1789–1802
10. Spikes JD (1986) Phthalocyanines as photosensitizers in biological systems and for the photodynamic therapy of tumors. Photochem Photobiol 43(6):691–699
11. Hanack M, Gul A, Hirsch A, Mandal BK, Subramanian LR, Witke E (1990) Synthesis and characterization of soluble phthalocyanines—structure–property relationship. Mol Cryst Liquid Cryst 187:365–382
12. Abramczyk H, Szymczyk I (2004) Aggregation of phthalocyanine derivatives in liquid solutions and human blood. J Mol Liq 110(1–3):51–56
13. Kuznetsova NA, Gretsova NS, Derkacheva VM, Kaliya OL, Lukyanets EA (2003) Sulfonated phthalocyanines: aggregation and singlet oxygen quantum yield in aqueous solutions. J Porphyr Phthalocyanines 7(3):147–154
14. Hanack M, Schmid G, Sommerauer M (1993) Chromatographic separation of the 4 possible structural isomers of a tetrasubstituted phthalocyanine-tekrakis(2-ethylhexyloxy)phthalocyaninatonickel (Ii). Angew Chem Int Ed Engl 32(10):1422–1424
15. Hanack M, Meng DY, Beck A, Sommerauer M, Subramanian LR (1993) Separation of structural isomers of tetra-tert-butylphthalocyaninatonickel(Ii). J Chem Soc Chem Commun 1:58–60
16. Leznoff CC, Hall TW (1982) The synthesis of a soluble, unsymmetrical phthalocyanine on a polymer support. Tetrahedron Lett 23(30):3023–3026
17. Leznoff CC (1989) Phthalocyanines: properties and applications, 1. VCH, New York
18. McCubbin I, Phillips D (1986) The photophysics and photostability of zinc(Ii) and aluminum(Iii) sulfonated naphthalocyanines. J Photochem 34(2):187–195
19. Huang TH, Rieckhoff KE, Voigt EM (1977) Spin-orbit effects in metalphthalocyanines. Chem Phys 19(1):25–33
20. Wu SK, Zhang HC, Cui GZ, Xu DN, Xu HJ (1985) A study on the ability of some phthalocyanine compounds for photogenerating singlet oxygen. Acta Chimi Sin 43(1):10–13
21. Cuellar EA, Marks TJ (1981) Synthesis and characterization of metallo and metal-free octaalkylphthalocyanines and uranyl decaalkylsuperphthalocyanines. Inorg Chem 20(11):3766–3770
22. Sakamoto K, Kato T, Ohno-Okumura E, Watanabe M, Cook MJ (2005) Synthesis of novel cationic amphiphilic phthalocyanine derivatives for next generation photosensitizer using photodynamic therapy of cancer. Dyes Pigm 64(1):63–71
23. Ng ACH, Li XY, Ng DKP (1999) Synthesis and photophysical properties of nonaggregated phthalocyanines bearing dendritic substituents. Macromolecules 32(16):5292–5298
24. Sener MK (2005) Synthesis of tetr(tricarbethoxy)- and tetra (dicarboxy)-substituted soluble phthalocyanines. J Porphyr Phthalocyanines 7:617–622
25. Duan WB, Smith K, Savoie H, Savoie H, Greenman J, Boyle RW (2005) Near IR emitting isothiocyanato-substituted fluorophores: their synthesis and bioconjugation to monoclonal antibodies. Org Biomol Chem 3(13):2384–2386
26. Hammer RP, Owens CV, Hwang SH, Sayes CM, Soper SA (2002) Asymmetrical, water-soluble phthalocyanine dyes for covalent labeling of oligonucleotides. Bioconjug Chem 13(6):1244–1252
27. Koval VV, Chernonosov AA, Abramova TV, Ivanova TM, Fedorova OS, Knorre DG (2000) The synthesis of a cobalt(II) tetracarboxyphthalocyanine–deoxyribooligonucleotide conjugate as a reagent for the directed DNA modification. Bioorganicheskaya Khimiya 26(2):118–125
28. Patonay G, Antoine MD, Devanathan S, Strekowski L (1991) Near-infrared probe for determination of solvent hydrophobicity. Appl Spectrosc 45(3):457–461
29. Demas JN, Crosby GA (1971) Measurement of photoluminescence quantum yields—review. J Phys Chem 75(8):991–1024
30. Fery-Forgues S, Lavabre D (1999) Are fluorescence quantum yields so tricky to measure? A demonstration using familiar stationery products. J Chem Educ 76(9):1260–1264
31. Davidson YY, Gunn BM, Soper SA (1996) Spectroscopic and binding properties of near-infrared tricarbocyanine dyes to double-stranded DNA. Appl Spectrosc 50(2):211–221
32. Keller TM, Price TR, Griffith JR (1980) Synthesis of phthalonitriles by nitro displacement. Synthesis–Stuttgart 8:613
33. Yanagisawa M, Korodi F, Bergquist J, Holmberg A, Hagfeldt A, Akermark B, Sun LC (2004) Synthesis of phthalocyanines with two carboxylic acid groups and their utilization in solar cells based on nanostructured TiO2. J Porphyr Phthalocyanines 8(10): 1228–1235
34. Negri RM, Zalts A, Roman EAS, Aramendia PF, Braslavsky SE (1991) Carboxylated zinc phthalocyanine, influence of dimerization on the spectroscopic properties—an absorption, emission, and thermal lensing study. Photochem Photobiol 53(3):317–322
35. Ogunsipe A, Chen JY, Nyokong T (2004) Photophysical and photochemical studies of zinc(II) phthalocyanine derivatives—effects of substituents and solvents. New J Chem 28(7):822–827
36. Darwent JR, Douglas P, Harriman A, Porter G, Richoux MC (1982) Metal phthalocyanines and porphyrins as photosensitizers for reduction of water to hydrogen. Coord Chem Rev 44(1):83–126
37. Li YF, Li SL, Jiang KE, Yang LM (2004) Synthesis and spectral property of novel phthalocyanines substituted with four azo group moieties on periphery of phthalocyanine ring. Chem Lett 33(11): 1450–1451
38. McKeown NB, Chambrier I, Cook MJ (1990) Synthesis and characterization of some 1,4,8,11,15,18,22,25-octa-alkyl-22,25-bis(carboxypropyl)phthalocyanines and 1,4,8,11,15,18-hexa-alkyl-22,25-bis(carboxypropyl)phthalocyanines. J Chem Soc Perkin Trans 1(4):1169–1177
39. Strickler SJ, Berg RA (1962) Relation between absorption intensity and fluorescence lifetime of molecules. J Chem Phys 37:814–822
40. Morley JO, Charlton MH (1995) Theoretical investigation of the structure and spectra of zinc phthalocyanines. J Phys Chem 99(7):1928–1934
41. Stillman M, Mack J, Kobayashi N (2002) Theoretical aspects of the spectroscopy of porphyrins and phthalocyanines. J Porphyr Phthalocyanines 6(4):296–300
42. Kobayashi N, Konami H (2001) Molecular orbitals and electronic spectra of benzo-fused and related porphyrin analogues. J Porphyr Phthalocyanines 5(3):233–255
43. Minor PC, Gouterman M, Lever ABP (1985) Electronic-spectra of phthalocyanine radical-anions and cations. Inorg Chem 24(12): 1894–1900
44. Gouterman M, Wagniere GH, Snyder LC (1963) Spectra of porphyrins: part II. Four orbital model. J Mol Spectrosc 11(1–6): 108–127
45. Keizer SP, Mack J, Bench BA, Gorun SM, Stillman MJ (2003) Spectroscopy and electronic structure of electron deficient zinc phthalocyanines. J Am Chem Soc 125(23):7067–7085
46. Huang D, Liu ES, Yang SL, Chen NS, Huang JL, Duan JP, Chen Y (2000) The monomer electronic spectra and fluorescence spectra of some metal phthalocyanines. Spectroscopy and Spectral Analysis 20(1):95–98
47. Cook MJ, Dunn AJ, Howe SD, Thomson AJ, Harrison KJ (1988) Octa-alkoxy phthalocyanine and naphthalocyanine derivatives—dyes with Q-band absorption in the far red or near-infrared. J Chem Soc Perkin Trans 1(8):2453–2458

48. Tackley DR, Dent G, Smith WE (2001) Phthalocyanines: structure and vibrations. Phys Chem Chem Phys 3(8):1419–1426
49. Rosa A, Baerends EJ (1994) Metal macrocycle interaction in phthalocyanines—density-functional calculations of ground and excited states. Inorg Chem 33(3):584–595
50. Wynne KJ (1984) Crystal and molecular structure of chloro (phthalocyaninato)gallium(Iii), Ga(Pc)Cl, and chloro(phthalocyaninato)aluminum(Iii), Al(Pc)Cl. Inorg Chem 23(26):4658–4663
51. Phillips D, Dhami S, Ostler R, Petrasek Z (2003) The dimerisation of phthalocyanines. Prog React Kinet Mech 28(4):299–420
52. Ogunsipe A, Nyokong T (2004) Effects of substituents and solvents on the photochemical properties of zinc phthalocyanine complexes and their protonated derivatives. J Mol Struct 689(1–2):89–97
53. Kobayashi N, Lever ABP (1987) Cation-induced or solvent-induced supermolecular phthalocyanine formation—crown-ether substituted phthalocyanines. J Am Chem Soc 109(24):7433–7441
54. Isago H (2003) Spectral properties of a novel antimony(III)–phthalocyanine complex that behaves like J-aggregates in non-aqueous media. Chem Commun 15:1864–1865
55. Li XY, Ng DKP (2001) Synthesis and spectroscopic properties of the first phthalocyanine–nucleobase conjugates. Tetrahedron Lett 42(2):305–309
56. Ogunsipe A, Nyokong T (2005) Photophysical and photochemical studies of sulphonated non-transition metal phthalocyanines in aqueous and non-aqueous media. J Photochem Photobiol A Chem 173(2):211–220
57. Martin PC, Gouterman M, Pepich BV, Renzoni GE, Schindele DC (1991) Effects of ligands, solvent, and variable sulfonation on dimer formation of aluminum and zinc phthalocyaninesulfonates. Inorg Chem 30(17):3305–3309
58. Slota R, Dyrda G (2003) UV photostability of metal phthalocyanines in organic solvents. Inorg Chem 42(18):5743–5750